28 August 1967 RSIC-689

DELAYED FRACTURE OF TITANIUM ALLOYS

by

M. Kh. Shorshorov
V. N. Meshcheriakov

Novye Issledovaniya Titanovykh Splavov,
Izdatel'stvo Nauka, 278-288 (1965)

Translated from the Russian

Translation Branch
Redstone Scientific Information Center
Research and Development Directorate
U. S. Army Missile Command
Redstone Arsenal, Alabama 35809

DELAYED FRACTURE OF TITANIUM ALLOYS

by
M. Kh. Shorshorov
and
V. N. Meshcheriakov

Results of delayed-fracture tests on an IMET-4 machine for VT6S, VT6, and VT14M T: alloys, for a Ti alloy with low Al and Zr content, and for a Ti alloy with 3.7-percent Al. The fracture behavior and brittle properties of these alloys are compared. The mechanism involved is discussed noting the role of intergrain forces and absorbed gases.

The main typical features in behavior of titanium and its alloys when tested for delayed fractures and the formation of cold cracks in welded seams have been considered in the papers of Shorshorov.[1, 2, 3]

Tests in accordance with the IMET-4 methods[4] have been carried out in order to disclose the mechanism of delayed fracturing in titanium alloys. Flat specimens 2 to 3 mm in thickness, made of the same metal or containing welded ST spots (Figure 1) were subjected at room temperature to the action of a constant tensile load; the plastic deformation was measured while the specimen was under load until its rupture. The delayed fracture of the metal in the zone near the seam was investigated by using an argon-arc torch with tungsten electrodes to melt the specimens at each side of a notch, so that the zone near the seam was located at the place occupied by the notch. This was immediately followed by installing the specimens in the stands of the machine and subjecting them to a specified load. While under load, the plastic deformation was estimated by the relative narrowing of the specimen at the neck of the notch, which was measured at certain intervals of time. The notch was needed not only to establish the place of rupture but also to form a two-axial stressed state.

Results of delayed-fracture tests had shown that a sizeable intergrain deformation (Table I) develops in alloys with low yield point (Ti + 3.7-percent Al, OT4-1) and with medium yield points (VT6S) and a low content of gases (0.12-0.3-percent O_2, 0.03-0.4-percent N_2, and 0.01-percent H_2). At the beginning of fracturing, the relative narrowing ψ_p of the cross section at the place of the notch may reach 25 to 70 percent of the narrowing ψ of the same specimens tested for static elongation. The minimum rupturing stress $\sigma_{p\,min}$ (along the initial cross section of the specimen) varies within 75 to 95 percent of the yield points of the alloys. The values ψ_p and $\sigma_{p\,min}$ are determined by the composition of the alloys, their structural state, and the size of the grains.

Table I. Characteristics of Resistance Offered by Titanium Alloys to Delayed Fracture, as per IMET-4 Method

Trademark of Alloys and Thickness of Specimens	Content of Gases			Place of Fracture	Properties at Static Elongation		Criterion of Resistance to Delayed Fracture			
	O	N	H		σ_p kg(force)/mm^2	δ, %	$\sigma_{p\,min}$ kg(force)/mm^2	t_p at $\sigma_{p\,min}$ days	ψ Prior to the Beginning of the Fracturing	ψ After the Fracturing
VT6S (4.56% Al, 3.36% V) 3mm	0.12	0.04	0.006	Main metal (after rolling and annealing at 600°)	122-129	24-26	97-98	12-20	17-19	32-34
	0.12	0.04	0.006	Zone near the seam	127-130	18-20	112-113	5-35	12-14	23-25
	0.1	0.04	0.002	Main metal (after rolling and annealing at 800°)	81-82	40-42	56-57	45-55	25-28	42-44
	0.1	0.04	0.002	Zone near the seam	82-83	35-37	61-62	70	25-26	40-41
	0.1	0.04	0.015	Main metal	82-83	31-32	53-54	3-4	18-19	33-34
	0.1	0.04	0.015	Zone near the seam	82-84	29-30	60-61	70	15-16	21-22
	0.29	0.04	0.0025	Main metal	100-102	38-39	74-75	70	20-21	34-35
	0.29	0.04	0.0025	Zone near the seam	113-114	27-28	82-83	70	16-17	22-23
Ti-Al-Zr, 3 mm	0.29	0.04	0.011	Main metal	103-104	16-20	71-72	40-50	12-13	17-18
Ti-Al-Zr, 3 mm	0.29	0.04	0.011	Zone near the seam	115-116	6-18	74-75	30-40	9-10	12-14
	0.29	0.04	0.014	Main metal	104-105	19-20	70-71	28-32	6-7	14-15
	0.29	0.04	0.014	Zone near the seam	111-113	20-21	79-80	30-34	15-16	20-22
	0.13-0.14	0.04	0.002	Main metal	87-94	26-32	68-69	0.3-1.0	15-17	32-39
	0.13-0.14	0.04	0.002	Zone near the seam	88-90	24-32	69-70	2.5-5.0	19-20	30-39
	0.45	0.04	0.002	Main metal	112-114	18-19	82-83	3-4	9-10	23-24
	0.45	0.04	0.002	Zone near the seam	113-116	18-24	84-85	4-7	7-8	20-21
Ti-3.7% Al, 2 mm	0.12	0.03	0.007	Main metal (after rolling and annealing at 600°)	83-84	39-43	80-81	10-15	14-16	23-25
	0.12	0.03	0.007	Zone near the seam	92-96	29-33	87-88	5-15	11-14	16-20
OT4-1 (1.75% Al, 1.06% Mn), 2 mm	0.13	0.048	0.005	Main metal after rolling	99-101	33-39	76-78	7-30	12-13	35-37
	0.13	0.048	0.005	Zone near the seam	98-100	32-38	72-75	10-60	10-11	24-26
OT4-1 (1.59% Al, 1.07% Mn) 3 mm *	0.13	0.04	0.003	Main metal (after rolling and annealing at 500°)	103-108	29-31	79-80	0.8-8	9-10	24-28
	0.13	0.04	0.003	Zone near the seam	104-108	24-25	81-83	1-30	6-8	18-23
	0.13	0.04	0.04	Main metal after rolling	102-104	6-8	52-53	0.04-1	0-1	0-2
VT6 (6% Al, 4% V), 3 mm	0.2	0.03	0.01	Main metal after rolling	146-151	7-9	124-126	32-38	0-2	0-3
	0.2	0.1	0.01	Main metal after rolling	160-165	2-4	103-104	0.8-7	0	0
	0.3-0.4	0.03	0.01	Main metal after rolling	143-146	0	55-56	0.8-30	0	0
	0.2	0.03	0.05	Main metal after rolling	142-148	1-2	91-93	0.1-7	0	0
VT14M (4.5% Al, 3.5% Mo), 3 mm	0.14	0.045	0.011	Zone near the seam (before welding quenched from 860°)	123-128	9-11	119-120	0.5-1	0	0
	0.14	0.045	0.011	Zone near the seam (before welding quenched from 860°, after welding quenched from 860° and aged at 500°, 16 hrs	138-142	6-8	131-132	1-5	5-7	11-13

*The specimens with notches (as in Figure 1) used also in testing delayed fracture.

The main metal with an α-structure when annealed after its rolling has a $\sigma_{p\ min}$ lower and a ψ_p higher than the metal of the zone near the seam, which has an α'-structure (see Table I, the alloys Ti-3.7-percent Al; OT4-1, 3mm thick; and VT6S). On the other hand a main metal not annealed after its rolling (alloy OT4-1, 2mm thick) may have an even higher $\sigma_{p\ min}$ than that of the metal in the zone near the seam. In such a case, the main metal has the structure of an α'-phase with fine textured grains that assure a higher resistance to delayed fracture.

The stepped appearance of the curves for the change in deformation with time (Figure 2) indicates the presence of a strong barrier-effect of the grain boundaries in titanium alloys having an α- and α'-structure. This is a property of all metals having a compact hexagonal lattice at room temperature, because they have only one plane for easy sliding.

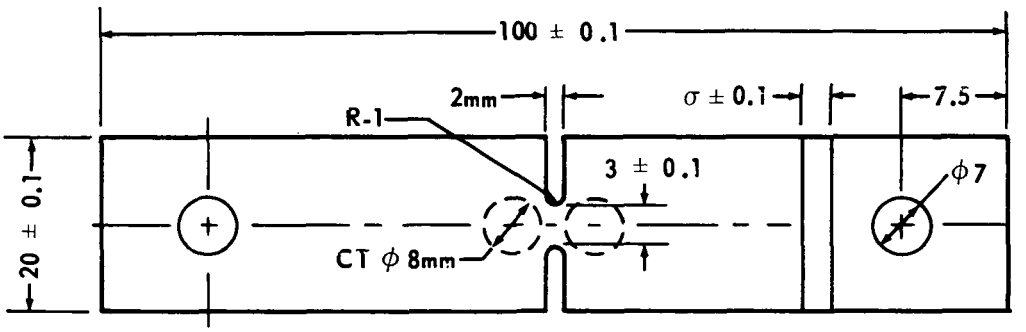

Figure 1. Specimen for Testing Delayed Fracture of Titanium Alloys in IMET-4 Machine

Plastic deformation increases insignificantly, or is totally absent, as long as the head-dislocations in the slip plane are unable to overcome in their path the barriers in the form of grains (or twinned grains). Compared with the main metal, the metal in the zone near the seam typically has a large number of such fluidity-stoppages and their following sections, with rapidly increasing deformation causing the formation of abrupt disruptions or dislocations upon overcoming the barriers. This phenomenon indicates a large degree of the local nature of the deformations in large-grain recrystallized metal; it is due to several causes: smaller number of grains with simultaneous favorable orientation of the plane with least resistance to slip (with respect to the direction of

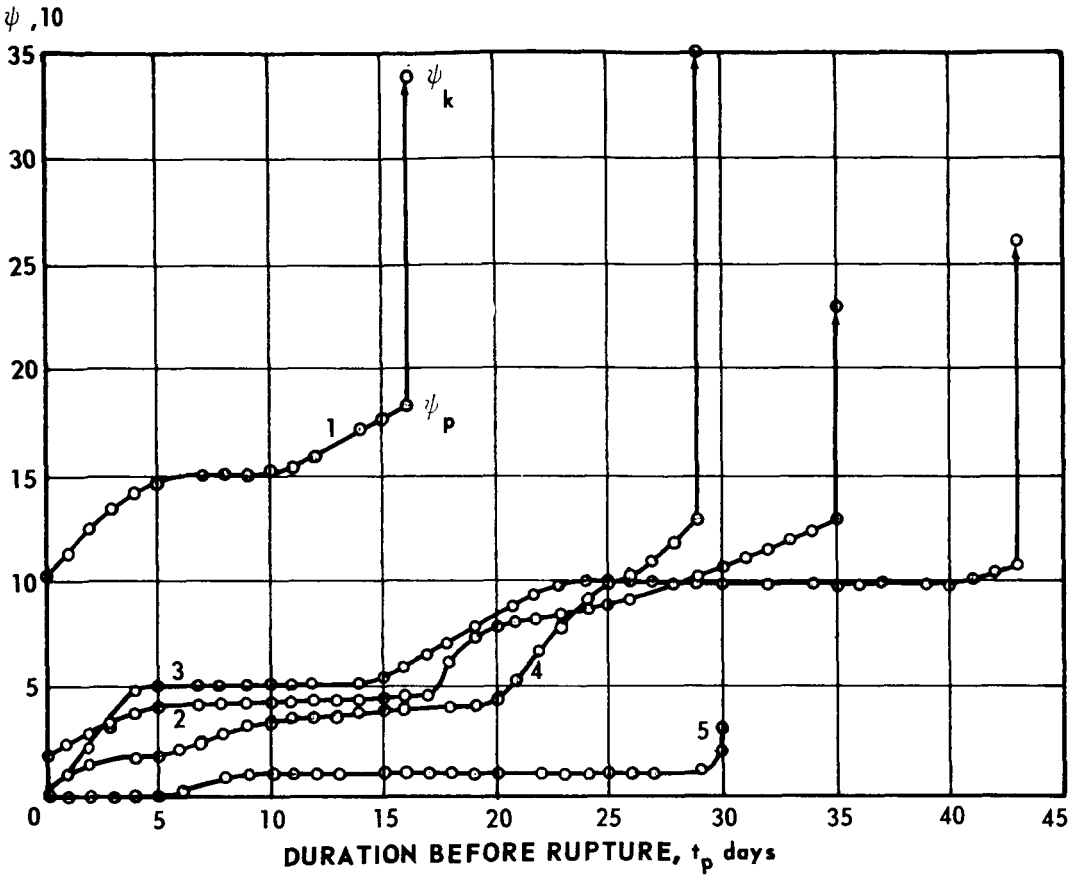

1) Main metal: VT6S alloy, $\sigma_{p\ min}$ = 98 kg (force)/mm^2
2) VT6S-alloy in zone near the seam $\sigma_{p\ min}$ = 113 kg/mm^2
3) Main metal of OT4-1 alloy, $\sigma_{p\ min}$ = 78 kg/mm^2
4) Zone near the seam of OT4-1 alloy, $\sigma_{p\ min}$ = 72 kg/mm^2
5) Zone near the seam of VT6-alloy, $\sigma_{p\ min}$ = 124 kg/mm^2

Figure 2. Change in Relative Narrowing of Transverse Section of Specimens at Place of Notch, Depending on Duration of Delayed Fracture Test of Titanium Alloys at Stresses Close to $\sigma_{p\ min}$

the effective effort), more effective action by boundaries with large angle as the barrier, etc. The same causes, and also the coarser character of the slip (mostly along ready-made strips for sliding formed as a result of thermal stresses during the welding), explain especially the lower ultimate values of ψ_p in the metal of the zone near the seam. Contrary to this, in a metal with

fine grains retaining the rolling texture despite the annealing, the deformation develops simultaneously in a large system of parallel slip planes.

The larger values of $\sigma_{p\ min}$ of a metal in the zone near the seam can be apparently explained by the larger resistance to shear of the metal with an α'-structure, its larger chemical homogeneity compared to that of the annealed structure of an α-phase, and also by the blocking effect of ready slip planes along the grain boundaries by the impurity atoms (O, N) during the cooling after welding. The last assumption is confirmed by the fact that a creep-test of commercial titanium at 150-300° discloses hardening. This effect is considered a phenomenon of deformation-aging. The dependence of strength and creep on time at stresses below the yield point, which is observed at room temperature, disappears at these higher temperatures.[5]

Moroz[6] was the first to detect a development of chemical heterogeneity in the α-phase of annealed titanium, particularly in such elements as iron, with limited solubility. Later the authors and I. Ya. Dzykovich had shown, with the aid of a local X-ray spectral analysis, that in an annealed alloy with 3.7-percent Al and 0.3-percent Fe, the grain boundaries and also the boundaries between the strips of the α-phase are richer in iron (up to 1-2 percent) and poorer in aluminum (up to 3.0-3.2 percent).

In alloys with high yield points, the macroscopic deformation in the zone near the seam is either too small or is not observed at all (VT14M). In VT6-alloy the deformation during the initial testing period becomes entirely localized along the grain boundaries and begins to develop inside the grain only after several days. As a case contrary to the alloys of the preceding group, in VT14M and VT6 alloys of the zone near the seam, the predominant places where cracks appear are the boundaries of the grains.

In the main metal, because of its fine grain structure, a fracture is always preceded by low plastic deformation, and cracks are formed both along the boundaries and in the body of the grains. The different character of the appearance of cracks in titanium alloys of these two groups is shown in Figure 3. The hardening and aging of VT14M alloy after its welding enables the metal in the zone near the seam to receive an appreciable deformation. This is helped by the appearance of sections of an α-phase poorer in β-stablizers, and also by a partial relaxation of the stresses.

The delayed-fracture test results testify to the very substantial effect of gases on the fracture mechanism of titanium alloys (Figure 4). Oxygen, nitrogen, and particularly hydrogen exert the most drastic unfavorable effects on the tendency to form cold cracks during the welding of α- and (α + β) alloys of titanium with a limited amount of α-phase.

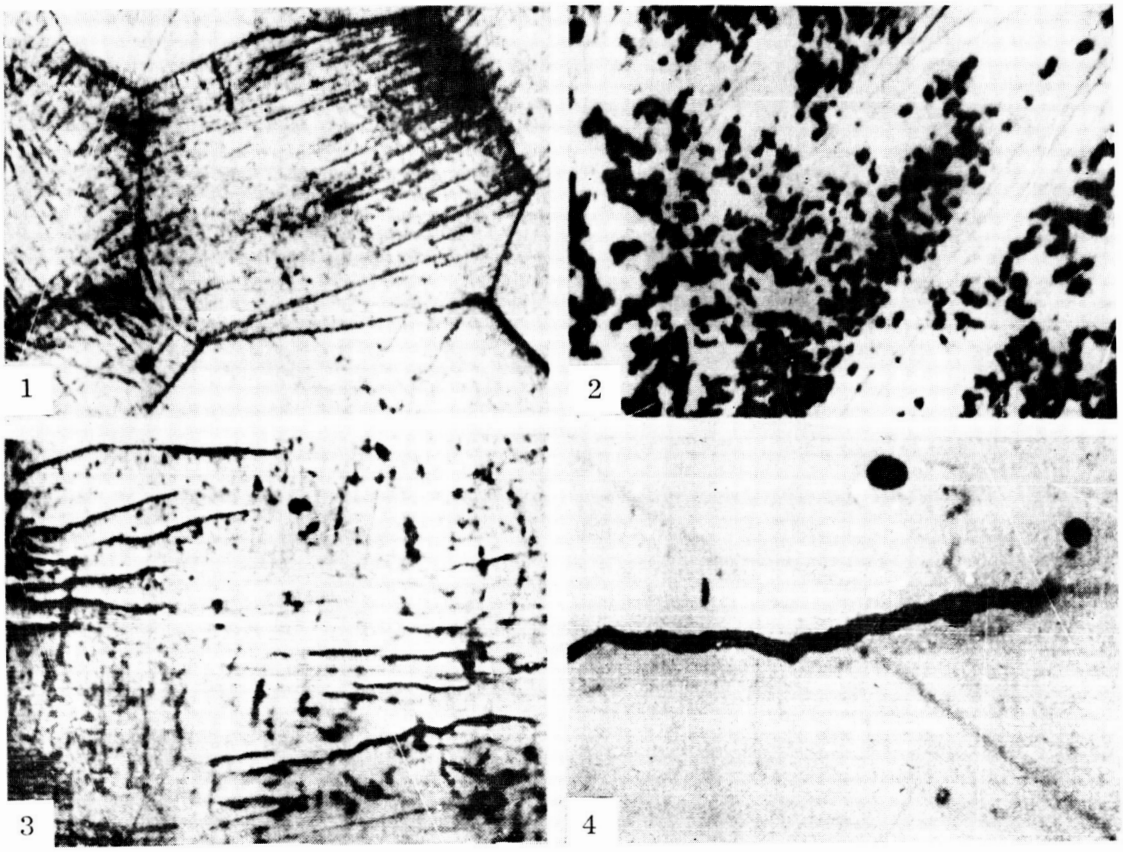

1) Cracks along grain boundaries in VT14M alloy (x 400)
2) σ cracks in slip-strip of OT4-1 alloy with deformation $\sigma \approx 10$ percent (x 900)
3) σ cracks in slip-strip of OT4-1 alloy with deformation $\sigma \approx 10$ percent (x 2000)
4) σ cracks in slip-strip of OT4-1 alloy with deformation $\sigma \approx 10$ percent (x 16,500)

Figure 3. Microscopic Cracks in Zone Near the Seam of Alloys with High (VT14M) and Medium (OT4-1) Yield Points Tested for Delayed Fracture

The example of a high-strength ($\alpha + \beta$) alloy VT6 shows that an increase in content of oxygen and nitrogen from 0.23 percent to 0.30-0.43 percent causes the metal in the zone near the seam to lose entirely its ability for intergrain deformation (see Figure 2 and Table I, where ψ_p and ψ_k are reduced from 2 to 3 percent to 0). This causes a drastic decrease in $\sigma_{p\ min}$ (respectively, from 124-126 to 103-104, and 55-56 kg (force)/mm^2), and reduces the time

until the fracture t_p from 2 to 0.8 days (see curves 1, 3, and 4, Figure 4). This is obviously due to the sharp increase in resistance to shear inside the grains, because of the blocking by dislocations located in slip planes already present.*

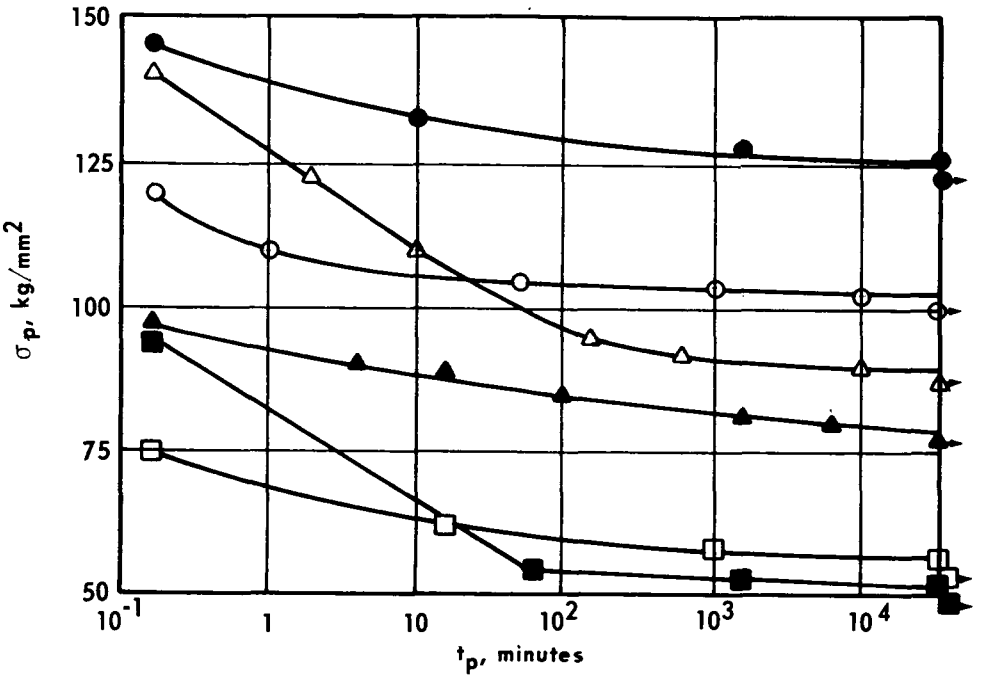

Figure 4. Change in Fracturing Stress σ_p, Depending on Time Until the Fracture of Metal in Zone Near the Seam for Different Contents of Gases in the Main Metal

Curve	Alloy	Content, %		
		0	N	H
1	VT6	0.2	0.03	0.01
2	VT6	0.2	0.03	0.05
3	VT6	0.2	0.10	0.01
4	VT6	0.3-0.4	0.03	0.01
5	OT4-1	0.13	0.04	0.003
6	OT4-1	0.13	0.04	0.04

Plastic deformation becomes concentrated along the borders of recrystallized grains which, because of the more defective structure, acquire the property of elastic-viscous flow. The fracturing becomes macroscopically brittle.

Oxygen has a different effect on the behavior of highly plastic alloys, particularly of α-alloys with a limited content of aluminum. For example, in

*In static elongation, this effect and also the blocking of dislocations in new strips serve to increase the yield point.

testing the delayed fracture of an alloy system Ti-Al-Zr, no reduction in $\sigma_{p\ min}$ and t_p takes place with the increase in content of oxygen from 0.13-0.14 percent to 0.45 percent (with a low concentration of hydrogen equal to 0.002 percent). On the contrary, $\sigma_{p\ min}$ increases from 68-69 to 82-84 kg/mm^2 and t_p increases from 0.3-5.0 to 3-7.0 days. At this, ψ_p is reduced from 15-20 percent to only 10-7 percent, i. e., to approximately one-half (Figure 5a, 5b, and Table I). This indicates that as the content of oxygen increases, the effectiveness of increasing blocking dislocations, the ability of intergrain deformation, and, consequently, the relaxation of stresses in these alloys still remains at a high level. Even an oxygen content as high as 0.45 percent proves to be insufficient for a transition to the macroscopically brittle, intergrain character of the fracturing.

The rate of creep in an alloy containing 0.13-0.14-percent oxygen is two or three times greater and changes much more drastically, depending on the applied stress, than in an alloy containing 0.45-percent oxygen (Figure 5c).

During the testing of highly plastic alloys acted upon by constant loads, the decrease in effective cross section of the specimen and the increase in effective stresses are so large that they lessen the accuracy of the comparative estimate of the ability of these alloys to resist delayed fracture from $\sigma_{p\ min}$ and ψ_p determined by the ratio to the initial cross section. Therefore, it is expedient to make the future tests for this type of alloy on machines in which the acting stress can be kept constant during the creep. Such tests are of special importance for analyzing the effect of small changes in content of alloying elements and impurities in alloys of identical systems.

An even sharper reduction in $\sigma_{p\ min}$ is obtained when the hydrogen content in OT4-1 alloy is increased from 0.003 percent to 0.04 percent (Figure 4, curves 5 and 6), and from 0.01 percent to 0.05 percent in VT6 alloy (curves 1 and 2), while the content of oxygen and nitrogen is relatively small (0.17 percent and 0.23 percent, respectively). In this case, at this $\sigma_{p\ min}$, the time until fracturing is also reduced considerably (from 1 to 0.04 and from 32 to 0.1 days, respectively). While for the VT6 alloy this may be primarily due to the adsorption effect of hydrogen, for the OT4-1 alloy it is also due to the added effect of hydride conversion. It is typical that in the PT4-1 alloy, with its clearly expressed hydride conversion, the reduction in $\sigma_{p\ min}$ and in t_p turn out to be more drastic, despite the fact that the metal in the zone near the seam retains a certain capacity for intergrain deformation. This is because the hydride conversion represents a substantial additional source of distortion not only

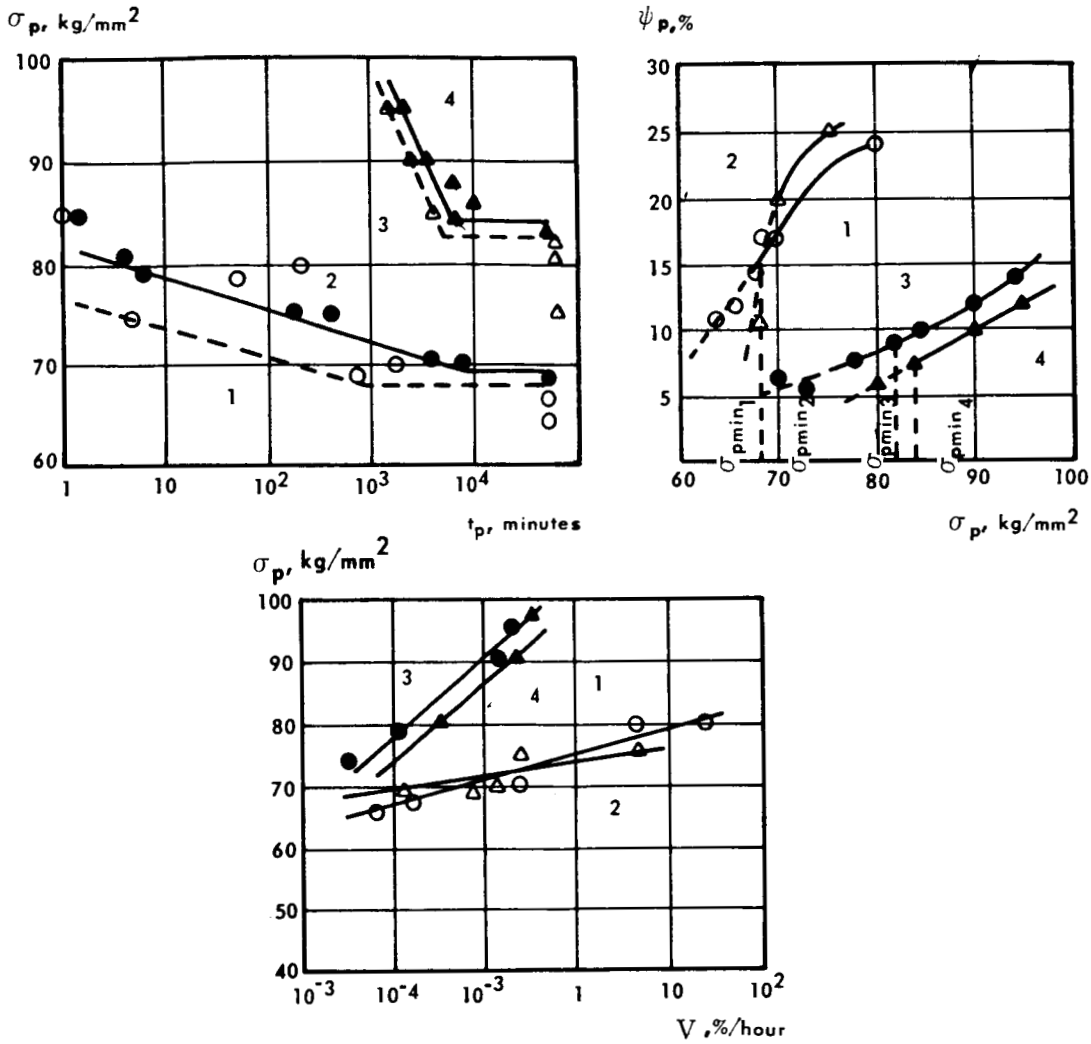

Figure 5. Relationship Between Fracturing Stress $\sigma_{p\,min}$, Time Until Fracturing t_p, Ultimate Creep ψ_p, and Rate of Creep v for Ti-Al-Zr System of Alloys Containing the Following Percentages of Oxygen:

1) Main metal 0.13 to 0.14-percent oxygen
2) Metal near the seam the same percent of oxygen
3) Main metal 0.45-percent oxygen
4) Metal near the seam, 0.45-percent oxygen

along the grain boundaries but also along the junction-planes $(10\overline{1}0)$. When the hydrides drop out, the slip-strips located along this plane may compete with the boundaries of recrystallized grains in degree of defectiveness of the structure.

Not excluded is the possibility that the boundaries separating the hydrides and the fragments of α- and α'-phases are the places for the formation of embryos of microcracks in the presence of hydrides.

In view of the known effect of the rate of cooling on the kinetics of hydride conversion and the dispersion of separated hydrides in the zone near the seam,[1] it was important to study this effect on an OT4-1 alloy with a high (0.04 percent) content of hydrogen. The content of oxygen plus the content of nitrogen was equal to 0.17 percent. The cooling rate was varied from 270 to 15 degrees per second by a preliminary heating of the specimens in a chamber with argon of prime composition. The results of these tests are shown in Table II.

Table II. Effect of Cooling Rate on Characteristics of Delayed Fracture of Metal in Zone Near the Seam of OT4-1 Alloy with 0.04-Percent Hydrogen

Cooling Rate ω_0, deg/sec	$\sigma_{p\ min}$ kg/mm^2	t_p, days	ψ_p, %	ψ_k, %	Average Grain Diameter, μ, mm
270	52-53	0.04-1	0-1	0-2	0.27
80	46-47	0.03-0.8	0	0	0.34
15	40-42	0.03-0.5	0	0	0.48

As the cooling rate decreases within these limits, there is a sharp drop in $\sigma_{p\ min}$ [by 11-12 kg (force)/mm^2], while t_p is reduced only by 15 minutes. Even at a cooling rate of 80 degrees per second, the metal in the zone near the seam has lost its capacity for plastic deformation (φ_p and $\varphi_k = 0$). The reduced resistance against delayed fracture apparently has two causes: coarse separation of hydrides and growth of grains. This confirms the expediency of using, if possible, more severe conditions for welding titanium alloys undergoing a hydride conversion.[1,7]

In more plastic alloys, such as in a Ti-Al-Zr system, the effect of reduced content of hydrogen (up to 0.015 percent) on the indicators of delayed fracture turns out to be less drastic. Shown in Figure 6 are the data on the effect of hydrogen within a range of 0.002-0.015 percent on the dependence on time of the strength of an alloy of this type containing the usual (0.1 percent) and a higher (0.29 percent) content of oxygen. For a content of 0.1-percent oxygen, the change in content of hydrogen within these limits reduces the $\sigma_{p\ min}$ of the main metal (by 2-2.5 kg/mm^2) very little. The reduction of $\sigma_{p\ min}$ is

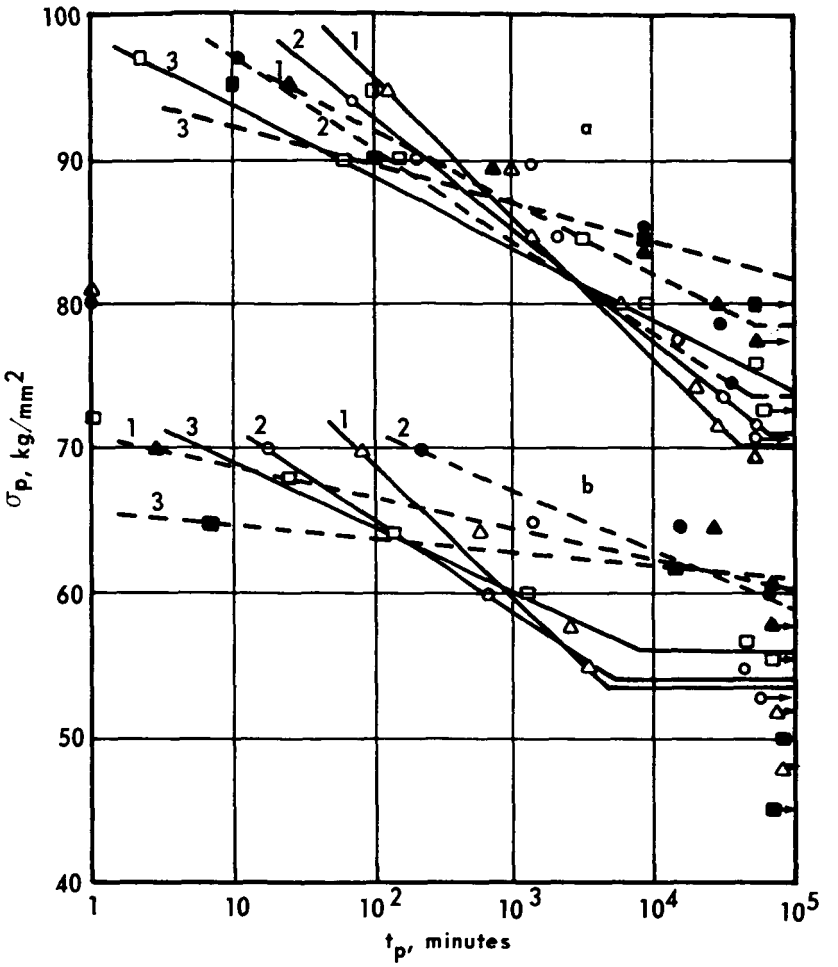

Figure 6. Relationship Between the Fracturing Stress and the Time Until the Fracture of Ti-Al-Zr System of Alloys with Various Contents of Hydrogen and Oxygen (Main Metal is Shown by Solid Lines, Broken Lines Indicate the Zone Near the Seam)

a. 0.29-percent oxygen: 1) 0.014-percent hydrogen,
2) 0.011-percent hydrogen,
3) 0.0025-percent hydrogen

b. 0.10-percent oxygen: 1) 0.015-percent hydrogen,
2) 0.010-percent hydrogen,
3) 0.002-percent hydrogen

more noticeable (by 3.5-4 kg/mm^2) but is not too large when the oxygen content is 0.29 percent. In both cases, ψ_p is also reduced but still remains at a fairly high level. In both metals in the zone near the seam, the resistance to delayed fracture is higher than in the main metal, which is apparently due to the partial

desorption of hydrogen during the welding.[7] At a higher content of oxygen, however, the effect of hydrogen on the $\sigma_{p\ min}$ of the zone near the seam is more substantial.

No conclusion can be drawn from the results of these tests about the expediency of increasing the earlier[1] allowable content of hydrogen (0.005-0.008 percent) in titanium alloys with an ultimate strength of 60-70 kg/mm^2, because a large saturation of oxygen in welded seams of inaccessible places during the welding of rigid structures is possible.

Similar investigations for alloys with high solubility of hydrogen (VT6, AT8) did not disclose a clear effect of the rate of cooling on delayed fracture, probably because of the absence of hydrides.

If the explanation of hydrogen brittleness is based, in particular, on the concepts about the effect of adsorption, then hydrogen can be considered a unique indicator of the time of formation of microcracks. The fact that an increase in the content of hydrogen reduces sharply the time t_p until the fracturing indicates that the origin of cracks begins during the relatively early stages of the tests, i. e., at relatively low degrees of deformation. Hydrogen, while adsorbed at the surface of these microcracks, contributes to their earlier development and to the brittle character of the fracture.

The soundness of this point of view is confirmed by the fact that even in very plastic metals (aluminum, copper, iron, and nickel) subjected to static elongation at room temperature, the formation of submicroscopic cracks begins at 7-10 percent of plastic deformation, long before the final destruction of the specimens.

In our earlier paper,[2] the fracture mechanism in titanium alloys having high yield points was explained by using the pattern of Zener that involves a visoelastic flow (slip) at a certain initial stage along the grain boundaries, followed by development of elastoplastic deformation in the volumes adjacent to the tops of the grain boundaries. As a result of this, the deformation becomes gradually less concentrated along the boundaries, and metal is enabled to receive a more noticeable intergrain deformation. An increased content of aluminum, β-stabilizing hardening elements, and impurities may localize the plastic deformation entirely along the boundaries of the grains. In such a case, the mechanism of forming microcracks in titanium alloys with a high yield point can be assumed to be the same as for tempered steels, including the substantial role played by vacancies.[2] Excessive concentrations of vacancies in titanium alloys, however, must be fewer because of the low volumetric effect and high temperature of the $\beta \rightarrow \alpha'$-conversion. This may be one of the reasons for the

longer duration of delayed fracture in titanium alloys with high yield points than in tempered steel. The main source of excessive concentrations of vacancies in titanium alloys is the quenching from high temperatures (the zone near the seam) and the large local deformation along the grain boundaries and along the junction-planes ($10\overline{1}0$) during the separation of the hydride phase.

Despite the low quantity of formed hydrides, the local character of their isolation and the large volumetric effect which accompanies the $\alpha \rightarrow \gamma$-conversion (three times higher than in martensite conversion in steels) are the factors that cause a high concentration of microstresses at the grain boundaries and the slip-planes. This is also helped by the fact that hydride conversions are developing mostly at lower temperatures.

Generally, when a noticeable plastic deformation in intergrain volumes develops at once or follows the slip along the grain-boundaries of titanium alloys, the analysis of the mechanism of formation of microcracks must be obviously based on modern dislocation models.

According to one of the widely used Zener-Straw models,[9] the initial formation of cracks (splinter type) takes place in sturdy obstacles (such as the boundaries of grains, twins, hydrides) blocking the slip-planes consisting of outer dislocations. However, the most realistic and more frequently confirmed in practice than the other models of formation of cracks in metals with compact hexagonal lattices are the models of Gilman[10] and Rozhanskiy.[11,12] According to these models, the formation of cracks is due to the nonlinearity of slip in slip-strips taking place near obstacles crowded by dislocations, or is a result of distortion of slip-planes when dislocations act in other effective slip-planes. The shift along the bent planes must bring with it normal stresses that cause the slip-planes to break away. These models are particularly important for metals in which, as in α-titanium, the slip-planes and the junction-planes coincide [base-planes ($10\overline{1}0$)]. The character of the formed cracks in OT4-1 alloy in microphotos obtained with the aid of optical and electronic microscopes (see Figure 3) correspond satisfactorily to the models of Gilman and Rozhanskiy.

The models of Cottrell, Orovan, and Friedel,[13,14] and of others, which are based on an analysis of phenomena taking place during the intersection of dislocations or when a slip-plane cuts a dislocation-net, are hardly suitable for our case because there are no intersecting slip-systems in hexagonal metals at low temperatures. The very slow development of deformation in titanium alloys tested for delayed fracture makes it possible to assume once more that excessive vacancies may play a substantial role in the mechanism of crack formation. Such hypotheses have been recently proposed and partly proven in many cases of static and alternating loading at room temperatures.[15] It is assumed that the main source of vacancies is the slip at which they are formed by the interaction of dislocations at the borders. However, this is valid only for metals with cubic

lattices; for metals with hexagonal lattices in which the slip-strips consist of partial dislocations, the mechanism of formation of vacancies still remains unexplained.

The above-mentioned mechanism of fracturing is most probable for titanium alloys with low and medium yield points. However, a simultaneous participation of both mechanisms, i. e., fractures in both along the grain boundaries and in the slip-planes, is assumed to be possible at certain contents of gases and alloying elements. For example, this may take place in high-strength (α + β)-alloys (VT6, VT14M) at high contents of oxygen and nitrogen if the resistance to shift along the grain boundaries and along the most easily sliding planes has a low limit, or at a high content of aluminum (AT8) where no hydride conversion takes place despite the relatively high content of hydrogen.

A comparative estimate of the resistance to delayed fracture in titanium alloys with low and medium yield points must be based on a comparison between the values of all three criteria ($\sigma_{p\ min}$, t_p, and ψ_p). The largest resistance will be in an alloy in which all three criteria are highest.

Of special importance for an alloy is a fairly high capacity for intergrain deformation (high φ_p) because it indicates the possibility of relaxation of the alloy's stresses without the danger of forming cracks. But a too-high tendency to "slippage" at relatively low stresses may turn out to be harmful from the standpoint of loss of stability and inadmissible change in shape and dimensions of the elementary welding structures.

In view of the above analysis of the possible mechanisms of delayed fracture, the tentative division of titanium alloys into those with low and high yield points is valid to the extent that the yield point is determined from the hardening of the solid solution by the impurity-atoms, because of their effective blocking of the dislocations.

Alloys with high yield points whose fracturing is macroscopically brittle should be evaluated by the total values of two criteria: $\sigma_{p\ min}$ and t_p.

According to the data obtained by testing delayed fracture in the IMET-4 machine, titanium alloys are arranged in this order: VT6S, alloys of the Ti-Al-Zr system with a low content of aluminum, Ti + 3.7-percent Al, OT4-1, followed by VT6 and VT14M. This indicates the advantages of alloying with elements that are isomorphic in the β-phase (V, Mo, etc.) instead of with elements forming β-eutectoids (Mn, Cr, Fe, etc). In the latter case, the alloys have a tendency to become cracked, apparently because of the separation of intermetalides in the slip-planes, which restricts their capacity for relaxation of the stresses caused by intergrain deformation.

LITERATURE CITED

1. M. Kh. Shorshorov and G. V. Nazarov, THE KINETICS OF PHASE-CONVERSION AND FORMATION OF COLD CRACKS IN WELDING TITANIUM AND ITS ALLOYS, Sb. Titan i Yego Splavy (Symposium: Titanium and Its Alloys), Academy of Sciences USSR, No. VII, 1962, p. 226.

2. M. Kh. Shorshorov, THE ROLE PLAYED BY VACANCIES IN MECHANISM OF DELAYED FRACTURE IN STEEL AND TITANIUM ALLOYS, Izv. AN SSSR, OTN, Metallurgiya i Toplivo (News of Academy of Sciences USSR Department of Technical Science, Metallurgy and Fuels), No. 4, 1962, p. 70.

3. M. Kh. Shorshorov, G. V. Nazarov, and V. V. Belov, SPECIAL FEATURES IN MECHANISM OF DELAYED FRACTURE AND FORMATION OF COLD CRACKS IN WELDING ALLOYS OF TITANIUM COMPARED WITH STEELS, Sb. Titan i Yego Splavy, Academy Sciences USSR, No. X, 1963, p. 284.

4. M. Kh. Shorshorov and V. V. Belov, EFFECT OF TECHNOLOGICAL FACTORS ON RESISTANCE TO DELAYED FRACTURE OF HARDENED STEELS NEAR THE SEAM (THE IMET-4 METHOD), Svarochnoye Poizvodstvo (Welding Production), No. 11, 1964.

5. L. S. Moroz, Yu. D. Khesin, and T. K. Marinets, INVESTIGATION OF SLIP AND PROLONGED HARDENING OF IRON AT LOW TEMPERATURES, Fizika Metallov i Metallovedeniye (Physics of Metals and Metallurgy), 1962, No. 13, 6, pp. 912-919.

6. L. S. Moroz, B. B. Chechulin, et al., TITAN I YEGO SPLAVY, Vol. 1, Sudpromgiz, 1960.

7. M. Kh. Shorshorov and G. V. Nazarov, SVARKA TITANA I YEGO SPLAVOV (Welding of Titanium and Its Alloys), Mashgiz, 1959.

8. I. A. Oding and Yu. P. Liberov, THE APPEARANCE OF SUBMICROSCOPIC CRACKS IN STATICALLY DEFORMED PLASTIC METALS, Izv. AN SSSR, OTN, Metallurgiya i Gornoye Delo (News of the Academy of Sciences, USSR, Department of Technical Science, Metallurgy and Mining), No. 2, 1964, pp. 85-91.

9. C. Zener, FRACTURING OF METALS, Cleveland, American Society of Metals, 1948.

10. I. I. Gilman, FRACTURE OF ZINC-MONOCRYSTALS AND BICRYSTALS, Trans. ASME, 1958, 212, No. 6, p. 192.

11. V. N. Rozhanskiy, ABOUT THE MECHANISM OF FORMED CRACKS IN CRYSTALS DURING PLASTIC DEFORMATION, Dokl. AN SSSR (Reports of the Academy of Sciences USSR), 1958, vol. 123, p. 648.

12. V. N. Rozhanskiy, CONCERNING THE CONDITIONS FOR APPEARANCE AND DEVELOPMENT OF CRACKS IN CRYSTALS, Fizika Tverdogo Tela (Solid State Physics), 1960, vol. 2, No. 6, pp. 1082-1088.

13. A. H. Cottrell, THEORY OF BRITTLE FRACTURE IN STEEL AND SIMILAR METALS, Trans. ASME, 1958, vol. 212, p. 192.

14. J. Friedel, LES DISLOCATIONS, Paris, 1956.

15. I. A. Oding and B. S. Ivanova, THE MECHANISMS OF FRACTURE OF METALS DUE TO FATIGUE, Trudy MET (Trans. of Institute of Metals), Academy of Sciences USSR, 1962, No. 13, pp. 3-28.

DOCUMENT CONTROL DATA - R & D

(Security classification of title, body of abstract and indexing annotation must be entered when the overall report is classified)

1. ORIGINATING ACTIVITY *(Corporate author)*
Redstone Scientific Information Center
Research and Development Directorate
U. S. Army Missile Command
Redstone Arsenal, Alabama 35809

2a. REPORT SECURITY CLASSIFICATION
Unclassified

2b. GROUP
N/A

3. REPORT TITLE
DELAYED FRACTURE OF TITANIUM ALLOYS
Novye Issledovaniya Titanovykh Splavov, Izdatel'stvo Nauka, 278-288 (1965)

4. DESCRIPTIVE NOTES *(Type of report and inclusive dates)*
Translated from the Russian

5. AUTHOR(S) *(First name, middle initial, last name)*
M. Kh. Shorshorov and V. N. Meshcheriakov

6. REPORT DATE	7a. TOTAL NO. OF PAGES	7b. NO. OF REFS
24 July 1967	22	15

8a. CONTRACT OR GRANT NO.	9a. ORIGINATOR'S REPORT NUMBER(S)
N/A	
b. PROJECT NO.	
N/A	RSIC-689
c.	9b. OTHER REPORT NO(S) *(Any other numbers that may be assigned this report)*
d.	

10. DISTRIBUTION STATEMENT
Distribution of this document is unlimited.

11. SUPPLEMENTARY NOTES	12. SPONSORING MILITARY ACTIVITY
None	Same as No. 1

13. ABSTRACT

Results of delayed-fracture tests on an IMET-4 machine for VT6S, VT6, and VT14M Ti alloys, for a Ti alloy with low Al and Zr content, and for a Ti alloy with 3.7-percent Al. The fracture behavior and brittle properties of these alloys are compared. The mechanism involved is discussed noting the role of intergrain forces and absorbed gases.

DD FORM 1 NOV 65 1473 REPLACES DD FORM 1473, 1 JAN 64, WHICH IS OBSOLETE FOR ARMY USE.

PAGES 17-20 BLANK NOT FILMED

14. KEY WORDS	LINK A		LINK B		LINK C	
	ROLE	WT	ROLE	WT	ROLE	WT
Delayed-fracture tests						
Deformation-aging phenomenon						
Macroscopic deformation						
Cold cracks						
Rate of creep						
Slip-planes						

(U) DISTRIBUTION

EXTERNAL

	No. of Copies
Air University Library ATTN: AUL3T Maxwell Air Force Base, Alabama 36112	1
U. S. Army Electronics Proving Ground ATTN: Technical Library Fort Huachuca, Arizona 85613	1
U. S. Naval Ordnance Test Station ATTN: Technical Library, Code 753 China Lake, California 93555	1
U. S. Naval Ordnance Laboratory ATTN: Library Corona, California 91720	1
Lawrence Radiation Laboratory ATTN: Technical Information Division P. O. Box 808 Livermore, California 94550	1
Sandia Corporation ATTN: Technical Library P. O. Box 969 Livermore, California 94551	1
U. S. Naval Postgraduate School ATTN: Library Monterey, California 93940	1
Electronic Warfare Laboratory, USAECOM Post Office Box 205 Mountain View, California 94042	1
Jet Propulsion Laboratory ATTN: Library (TDS) 4800 Oak Grove Drive Pasadena, California 91103	2
U. S. Naval Missile Center ATTN: Technical Library, Code N3022 Point Mugu, California 93041	1
U. S. Army Air Defense Command ATTN: ADSX Ent Air Force Base, Colorado 80912	1
Central Intelligence Agency ATTN: OCR/DD-Standard Distribution Washington, D. C. 20505	4
Harry Diamond Laboratories ATTN: Library Washington, D. C. 20438	1
Scientific & Tech. Information Div., NASA ATTN: ATS Washington, D. C. 20546	1
U. S. Atomic Energy Commission ATTN: Reports Library, Room G-017 Washington, D. C. 20545	1
U. S. Naval Research Laboratory ATTN: Code 2027 Washington, D. C. 20390	1
Weapons Systems Evaluation Group Washington, D. C. 20305	1
John F. Kennedy Space Center, NASA ATTN: KSC Library, Documents Section Kennedy Space Center, Florida 32899	2
APGC (PGBPS-12) Eglin Air Force Base, Florida 32542	1
U. S. Army CDC Infantry Agency Fort Benning, Georgia 31905	1
Argonne National Laboratory ATTN: Report Section 9700 South Cass Avenue Argonne, Illinois 60440	1
U. S. Army Weapons Command ATTN: AMSWE-RDR Rock Island, Illinois 61201	1
Rock Island Arsenal ATTN: SWERI-RDI Rock Island, Illinois 61201	1
U. S. Army Cmd. & General Staff College ATTN: Acquisitions, Library Division Fort Leavenworth, Kansas 66027	1
Combined Arms Group, USACDC ATTN: Op. Res., P and P Div. Fort Leavenworth, Kansas 66027	1
U. S. Army CDC Armor Agency Fort Knox, Kentucky 40121	1
Michoud Assembly Facility, NASA ATTN: Library, I-MICH-OSD P. O. Box 29300 New Orleans, Louisiana 70129	1
Aberdeen Proving Ground ATTN: Technical Library, Bldg. 313 Aberdeen Proving Ground, Maryland 21005	1
NASA Sci. & Tech. Information Facility ATTN: Acquisitions Branch (S-AK/DL) P. O. Box 33 College Park, Maryland 20740	5
U. S. Army Edgewood Arsenal ATTN: Librarian, Tech. Info. Div. Edgewood Arsenal, Maryland 21010	1

	No. of Copies
National Security Agency ATTN: C3/TDL Fort Meade, Maryland 20755	1
Goddard Space Flight Center, NASA ATTN: Library, Documents Section Greenbelt, Maryland 20771	1
U. S. Naval Propellant Plant ATTN: Technical Library Indian Head, Maryland 20640	1
U. S. Naval Ordnance Laboratory ATTN: Librarian, Eva Liberman Silver Spring, Maryland 20910	1
Air Force Cambridge Research Labs. L. G. Hanscom Field ATTN: CRMXLR/Stop 29 Bedford, Massachusetts 01730	1
Springfield Armory ATTN: SWESP-RE Springfield, Massachusetts 01101	1
U. S. Army Materials Research Agency ATTN: AMXMR-ATL Watertown, Massachusetts 02172	1
Strategic Air Command (OAI) Offutt Air Force Base, Nebraska 68113	1
Picatinny Arsenal, USAMUCOM ATTN: SMUPA-VA6 Dover, New Jersey 07801	1
U. S. Army Electronics Command ATTN: AMSEL-CB Fort Monmouth, New Jersey 07703	1
Sandia Corporation ATTN: Technical Library P. O. Box 5800 Albuquerque, New Mexico 87115	1
ORA(RRRT) Holloman Air Force Base, New Mexico 88330	1
Los Alamos Scientific Laboratory ATTN: Report Library P. O. Box 1663 Los Alamos, New Mexico 87544	1
White Sands Missile Range ATTN: Technical Library White Sands, New Mexico 88002	1
Rome Air Development Center (EMLAL-1) ATTN: Documents Library Griffiss Air Force Base, New York 13440	1
Brookhaven National Laboratory Technical Information Division ATTN: Classified Documents Group Upton, Long Island, New York 11973	1
Watervliet Arsenal ATTN: SWEWV-RD Watervliet, New York 12189	1
U. S. Army Research Office (ARO-D) ATTN: CRD-AA-IP Box CM, Duke Station Durham, North Carolina 27706	1
Lewis Research Center, NASA ATTN: Library 21000 Brookpark Road Cleveland, Ohio 44135	1
Systems Engineering Group (RTD) ATTN: SEPIR Wright-Patterson Air Force Base, Ohio 45433	1
U. S. Army Artillery & Missile School ATTN: Guided Missile Department Fort Sill, Oklahoma 73503	1
U. S. Army CDC Artillery Agency ATTN: Library Fort Sill, Oklahoma 73504	1
U. S. Army War College ATTN: Library Carlisle Barracks, Pennsylvania 17013	1
U. S. Naval Air Development Center ATTN: Technical Library Johnsville, Warminster, Pennsylvania 18974	1
Frankford Arsenal ATTN: C-2500-Library Philadelphia, Pennsylvania 19137	1
Div. of Technical Information Ext., USAEC P. O. Box 62 Oak Ridge, Tennessee 37830	1
Oak Ridge National Laboratory ATTN: Central Files P. O. Box X Oak Ridge, Tennessee 37830	1
Air Defense Agency, USACDC ATTN: Library Fort Bliss, Texas 79916	1
U. S. Army Air Defense School ATTN: AKBAAS-DR-R Fort Bliss, Texas 79906	1

	No. of Copies
U. S. Army CDC Nuclear Group Fort Bliss, Texas 79916	1
Manned Spacecraft Center, NASA ATTN: Technical Library, Code BM6 Houston, Texas 77058	1
Defense Documentation Center Cameron Station Alexandria, Virginia 22314	20
U. S. Army Research Office ATTN: STINFO Division 3045 Columbia Pike Arlington, Virginia 22204	1
U. S. Naval Weapons Laboratory ATTN: Technical Library Dahlgren, Virginia 22448	1
U. S. Army Engineer Res. & Dev. Labs. ATTN: Scientific & Technical Info. Br. Fort Belvoir, Virginia 22060	2
Langley Research Center, NASA ATTN: Library, MS-185 Hampton, Virginia 23365	1
Research Analysis Corporation ATTN: Library McLean, Virginia 22101	1
U. S. Army Tank Automotive Center ATTN: SMOTA-RTS.1 Warren, Michigan 48090	1
Hughes Aircraft Company Electronic Properties Information Center Florence Ave. & Teale St. Culver City, California 90230	1
Atomics International, Div. of NAA Liquid Metals Information Center P. O. Box 309 Canoga Park, California 91305	1
Foreign Technology Division ATTN: Library Wright-Patterson Air Force Base, Ohio 45400	1
Clearinghouse for Federal Scientific and Technical Information U. S. Department of Commerce Springfield, Virginia 22151	1
Foreign Science & Technology Center, USAMC ATTN: Mr. Shapiro Washington, D. C. 20315	3
National Aeronautics & Space Administration Code USS-T (Translation Section) Washington, D. C. 20546	2

	No. of Copies
INTERNAL	
Headquarters U. S. Army Missile Command Redstone Arsenal, Alabama 35809	
ATTN: AMSMI-D	1
AMSMI-XE, Mr. Lowers	1
AMSMI-XS	1
AMSMI-Y	1
AMSMI-R, Mr. McDaniel	1
AMSMI-RAP	1
AMSMI-RBLD	10
USACDC-LnO	1
AMSMI-RB, Mr. Croxton	1
AMSMI-RBT	8
National Aeronautics & Space Administration Marshall Space Flight Center Huntsville, Alabama 35809	
ATTN: MS-T, Mr. Wiggins	5
R-P&VE-MMC, Mr. Lowery	1